Octahedral tilt phases in perovskite-like crystals with slabs containing an even number of octahedral layers

1994 J. Phys.: Condens. Matter 6 8219

(http://iopscience.iop.org/0953-8984/6/40/013)

J. Phys.: Condens. Matter 6 (1994) 8219–8235. Printed in the UK

Octahedral tilt phases in perovskite-like crystals with slabs containing an even number of octahedral layers

K S Aleksandrov†‡ and J Bartolomé‡

† L V Kirensky Institute of Physics, Russian Academy of Sciences, Siberian Branch, 660036 Krasnoyarsk, Russia

‡ Instituto de Ciencia de Materiales de Aragón, CSIC-Universidad de Zaragoza, 50009 Zaragoza, Spain

Received 4 March 1994, in final form 3 June 1994

Abstract. The possible combinations of different octahedral tilts are considered for layered crystals having an even number of octahedral layers in perovskite-like slabs. A simple method to determine the resultant space-group symmetry is proposed, and the distorted phases are enumerated, both for a single kind of tilt around axes of the initial structure $G_0 = I4/mmm$ and for superpositions of different tilts in the slabs. Some of the tilt systems correspond to symmetry changes due to definite irreducible representations of G_0. In the single-layered crystals, $l = 1$, A_2BX_4, some of the representations correspond to lattice modes observed experimentally. No such modes have been found yet for even-layered ($l = 2n$) crystals. A comparison with known experimental data is performed. The data obtained can be used for the proposition of 'trial models' in the course of structural analysis of related crystals.

1. Introduction

Perovskites and perovskite-like crystals consist of quite regular octahedra sharing corners. Structural phase transitions (PTs) in which tilts of these octahedra around their three diagonals occur have been widely investigated during the last two decades. Most attention has been paid to PTs taking place in the extensive families of crystals such as those of ABX_3 of perovskite type [1–3], $A_2BB'X_6$ of elpasolite type [3, 4] and their relatives $A_2\square BX_6$ of K_2PtCl_6 type and $\square_2BB'X_6$ of ReO_3 type [3, 5, 6]. Here A and B are cations of the proper size and valency, and $\square$ are vacancies in the A or B sites of the lattice of octahedra. As has been shown in previous papers, many complex sequences of structural PTs in these families can be described as superpositions of different coupled tilts of the octahedral BX_6 groups. The resultant space-group symmetry of the possible distorted phases has been obtained and it has been shown that such a scheme can describe all experimentally observed symmetry changes at successive PTs as temperature or pressure are varied.

Similar crystallographic work has been done also for those crystal structures in which the main feature of the perovskites, namely the square layers of corner-linked BX_6 octahedra, is preserved. These are the ABX_4 crystals of $TlAlF_4$ type and A_2BX_4 crystals of K_2MgF_4 type [7–12]. Both structures contain single layers of perovskite-like octahedra. The different distorted phases obtained by superposition of the three kinds of tilt have been tabulated in these papers. Moroever, by means of group-theoretical analysis, it has been shown that some PTs due to tilts are determined by irreducible representations (irreps) of the initial space groups G_0. The librational phonon modes involving the octahedra in the crystal lattices transform in accordance to these irreps, and they correspond in many cases to the

0953-8984/94/408219+17$19.50

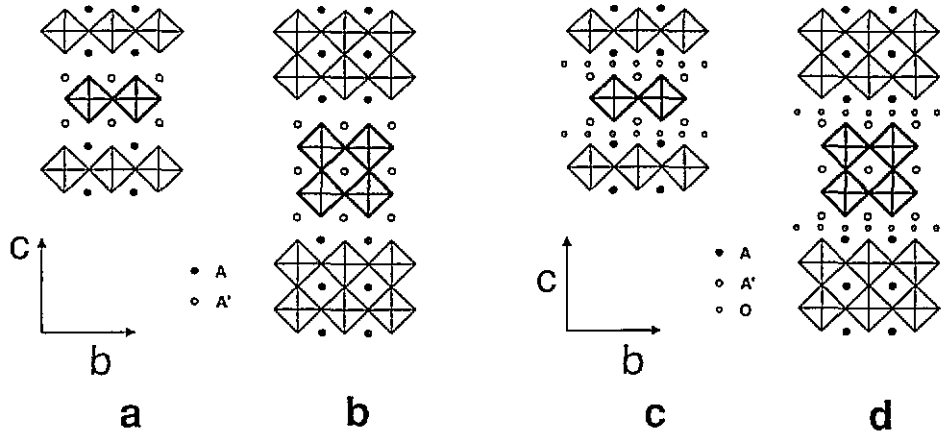

Figure 1. Ideal tetragonal perovskite-like structures of the first members of the Ruddlesden–Popper (a, b) and Aurivillius (c, d) series projected on the $(100)_o$ plane of $G_o = I4/mmm$ of A_2BX_4 and A_2BX_6 types.

soft modes that condense at the PTs. Some examples are $RbAlF_4$ [13], Rb_2CdCl_4 [14, 15], and La_2CuO_4 [16].

In some cases sequences of PTs take place, as in La_2CuO_4, where the initial high-temperature tetragonal phase distorts successively to orthorhombic and then to tetragonal symmetry as the temperature is lowered. This is due to the appearance and variation of the same tilts giving rise to the same two-component order parameter [9, 10]. The symmetry of the distorted phases of A_2BX_4, obtained by two independent groups and compared to the available experimental data prior to 1988, is contained in [12].

The research on perovskite-like layered crystals became much more active because of the discovery of high-temperature superconductivity (HTSC) in La_2CuO_4, and Bi_2 and Tl_2 series of anion-deficient layered compounds. Some of the crystals are formed by single layers of octahedra and others by slabs of l layers of octahedra, with $l = 2n$ and $l = 2n+1$. These slabs alternate with NaCl-type, CaF_2-type, or more complex intermediate layers. Two well known families of crystals with general formula $AX(A'BX_3)_l$ for Ruddlesden–Popper phases [17] and $A_2O_2(A'_{l-1}B_lX_{3l+1})$ for Aurivillius phases [18] are often met in oxides and halogenides (X = F, Cl). The structures of the first two members of both series are shown in figure 1. In fact, these two series are also the forefathers of some HTSC series. In addition, there are many examples of structural, ferroelectric, antiferroelectric and antiferromagnetic PTs in crystals belonging to these series.

The first members of the series correspond to the structures of K_2MgF_4 and Bi_2NbO_5F types. The crystallographic analysis of the PTs in terms of octahedral tilts for A_2BX_4 crystals is also applicable to the A_2BX_6 crystals of Bi_2NbO_5F type. In both series the initial space-group symmetries are the same: $G_o = I4/mmm$ for $l = 1$, $l = 2n$, $l = 2n + 1$. It is easy to show that the symmetry of the distorted phases listed earlier for A_2BX_4 [9, 12] does not change when the structures contain perovskite-like slabs with $l = 2n + 1$, although it is necessary to make some additions to the published tables. On the other hand, for structures where the perovskite-like slabs consist of an even number of octahedral layers ($l = 2n$), a new symmetry analysis of the distortions due to tilts is needed. This is the main purpose of the paper. The method of crystallographic analysis and the kinds of simple tilt are described in section 2; the main results of the analysis and some new (theoretical) cases of so called

distortional polytypism can be found in tables 1 and 2 and figures 5 and 6 (section 3). A comparison with known experimental data is made and possible ways to use the results obtained for the structural analysis of layered crystals are discussed in section 4.

2. Method of analysis; kinds of tilt

The problem of listing all possible symmetry changes of crystal structure of an even-layer slab, under the assumption that symmetry lowering is due to modes involving rotations of the octahedra, will be first addressed. As previously done for other cases [4, 8–10], to determine the space group of the distorted phase, G_i, we just depict the structure of the distorted phase and check the resulting symmetry elements. As previously done for other cases [4, 8–10], we just depict the structure of a distorted phase and then perform a direct determination of the space group G_i. Applying an additional simplification of the problem (see below, figure 2), it is rather easy to determine the symmetry elements of the distorted structure, not only for the simple cases of single tilts but also in the cases where superpositions of different distortions (different kinds of tilt) takes place. In some perovskite-like families of crystals the distortions due to tilts have also been analysed with the same method [8, 10], and the results have often been confirmed experimentally. As earlier, it will be assumed below, as a first approximation, that for small tilts the BX_6 octahedra do not undergo further deformations.

Complex distortions are treated either as superpositions of the same kind of tilt but around different axes of the prototype structure, or of different kinds of tilt. We restrict ourselves here to cases when only one kind of tilt can occur around any axis of G_o. For simplicity, the A cations will be eliminated from the pictures, but we shall remember that their positions should be compatible with their site type within the resulting group G_i.

Another method to solve the problem of the G_i symmetry in A_2BX_4-type crystals was used by Hatch and Stokes [11, 12]. These authors have developed a computer program to determine the subgroups of G_o resulting both from single irreps of G_o and from the direct product of two irreps $\tau_i \otimes \tau_j$ corresponding to octahedral tilts in G_o. This method is theoretically more rigorous but it needs the analysis of direct products of irreps for the cases of coupled order parameters. Moreover, it is not easy to imagine the real changes of the atomic positions in G_i using only those irreps. Both methods lead to the same changes in symmetry, as has been shown many times [10, 12], and their combination gives the most clear and rigorous results [12].

For layered perovskite-like crystals of ABX_4 and A_2BX_4 types it was shown that three kinds of tilt are possible in a single square layer of the corner-linked octahedra. These are tilts around an axis normal to the layer plane, which will be labelled Ψ tilts (figure 2(c)) (they were previously called θ ones), and two kinds of tilt (Ψ and Φ), which can appear around the a_0 and/or b_0 axes of G_o. For Ψ tilts around b_0 all octahedra in a column along b_0 are turned in the same direction (figure 2(a)). The distortion of a layer (or slab) is denoted ($0\Psi0$): Ψ tilts along b_0, and the ($\Psi00$) distortion is an equivalent one. For two simultaneous Ψ tilts along both a_0 and b_0 axes the symbol ($\Psi\Psi0$) is used when both tilts are equal and the symbol ($\Psi_1\Psi_20$) for non-equal tilts. The Φ tilts are characterized by alternating angles of octahedral tilts along the rotation axis. Figure 2(b) corresponds to a ($0\Phi0$) distortion of a layer. ($\Phi\Phi0$) and ($\Phi_1\Phi_20$) distortions are also possible.

When A_2BX_4-type crystals have been analysed the distortions of G_o have been introduced by a double symbol, which represents the tilt systems in both layers (slabs), shifted in G_o by $1/2(a_0+b_0+c_0)$. For example, the distortions ($\Phi00$)($\Phi00$) and ($\Phi00$)($0\Phi0$)

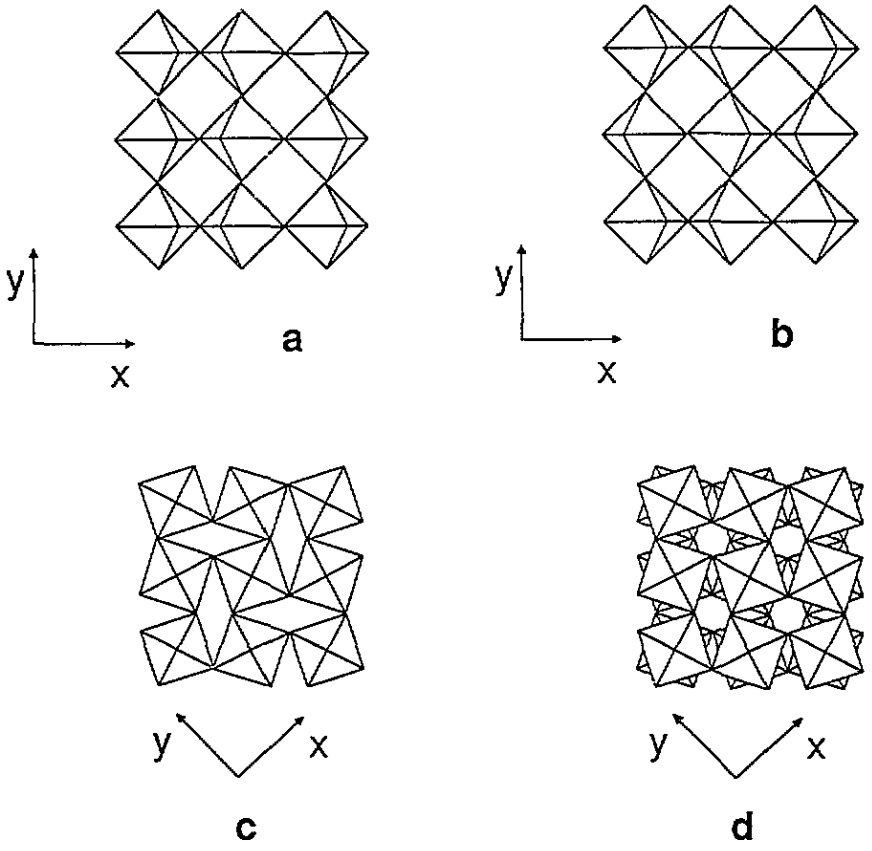

Figure 2. Four kinds of tilt in layers and slabs of corner-linked octahedra: (a) $(0\Psi 0)$; (b) $(0\Phi 0)$; (c) $(00\Psi_z)$; (d) $(00\Phi_z)$. The first three can appear in single-layered crystals of A_2BX_4 and A_2BX_6 types.

are distinguished by the different axes of equal tilts (and by the G_i symmetry of course). These axes are parallel to a_0 in the first case and mutually orthogonal in the second one.

When the G_0 structure contains octahedral slabs ($l \neq 1$) a fourth kind of tilt can exist: a Φ-tilt around the main axis of G_0 (figure 2(d)). This leads to different space groups in crystals with even layers $l = 2n$ because $(00\Phi_z)$ tilts (Φ tilts along the c axis) do not keep the mirror plane orthogonal to the main axis of G_0. On the other hand, in the case of Ψ and Φ tilts the same mirror plane (between the octahedral layers in the slabs with $l = 2n$) is maintained. The situation is exactly opposite to the slabs with $l = 2n + 1$ where the m plane is lost for Ψ and Φ tilts but exists for $(00\theta) = (00\Phi_z)$ ones. (It is worthwhile to mention here again that in previous papers the symbol θ was used instead of Ψ_z). One should remember also that Ψ and Ψ_z, Φ and Φ_z tilts are tilts of the same kind, *but tilts in both pairs inevitably belong to different irreps of* G_0. *It was shown earlier for* crystals with $l = 1$ [9, 12] that some distortions due to Ψ_z and Φ tilts are determined by two-dimensional irreps $\tau_7(X_2^+)$, $\tau_3(X_3^+)$ and $\tau_5(X_4^+)$ of G_0 in Kovalev, and Miller and Love notations [19, 20]. It will be shown later that a similar situation takes place in the crystals under present consideration.

3. Results of the crystallographic analysis for crystals with slabs containing an even number of octahedral layers

Independently of the number of octahedral layers in the slabs, the initial space group for both series of crystals (figure 1) is $G_o = D_{4h}^{17}$—$I4/mmm$ ($Z = 2$), where the slabs are shifted by half of the body diagonal of the I-centred unit cell. The (001) projection of superimposed slabs is shown in figure 3(a). The octahedra of the first (upper) slab are depicted by full lines and those of the second (lower) one at $z = 1/2c_0$ by broken lines. The A cations were omitted from the pictures here and below.

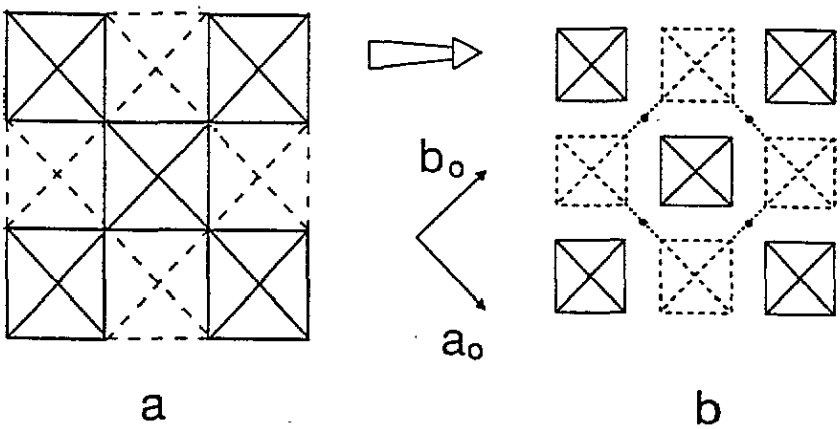

Figure 3. The method for simplification of the crystallographic analysis. The (001) projection of two neighbour slabs; A and A′ cations are omitted. The octahedra of the upper layer are drawn in full lines, those of the lower slab by broken lines. (a) Real structure; (b) simplified octahedral structure obtained by contracting all octahedra with respect to their centres. The unit cell of G_o is shown by dotted lines. The dots between octahedra correspond to the points of linkage in the real structure.

It becomes clear from inspection of figure 3(a) that the introduction of octahedral tilts will lead to further complications of the picture, and that the determination of the resulting symmetry will be a sophisticated problem. Therefore, an artificial method to simplify the problem was used. Each octahedron was contracted by half with respect to its centre (figure 3(b)). The points between the contracted octahedra in this figure mark the contact points of the octahedral vertices. This method simplifies the conception of the structure and does not change the symmetry of the G_o phase.

With this artificially simplified 'structure' it is much easier to introduce any kinds of tilt and consider their superpositions. Of course it is necessary to remember that octahedra are corner linked in both slabs. Therefore the phases of tilts in the neighbouring octahedra should correspond to the ones in the linked slab for each definite kind of tilt (Ψ, Φ, Ψ_z, Φ_z).

3.1. Tilts of the $(00\Psi_z)$ *kind*

These are determined by the two-dimensional $\tau_7(X_2^+)$ irrep of the K_{13} star of G_o [12]. Therefore three different distortions due to Ψ_z tilts may appear in the structure. The simplest distortion is shown in figure 4(a): the Ψ_z tilts are equal in both slabs: $(00\Psi_z)(00\Psi_z)$ and the distorted structure belongs to the space group D_{2h}^{18}—$Bbcm$ with $Z = 4$ and unit-cell

parameters $a = \sqrt{2}a_0$, $b = \sqrt{2}b_0$, $c = c_0$. Although the standard symbol of the group—*Cmca*—is used in table 1, the order of the unit-cell parameters is changed there. If the PT is $D_{4h}^{17} \rightarrow D_{2h}^{18}$, then only one component of the two-component order parameter, for example $(0, \eta)$ will appear. When the signs of the Ψ_z tilts in any slab are changed, the space group of G_i is the same, but the unit cell is centred in another $[110]_0$ plane (this corresponds to the $(\eta, 0)$ component of the order parameter). If the two distortions are superimposed, the values of the Ψ_z tilts in one of the slabs are doubled and compensate to zero on the other: $(002\Psi_z)(000)$. The coefficient will be omitted from table 1 in this case. The order parameter has both components identical: (η, η). The third case (η_1, η_2) with non-equal tilts in the slabs leads to other changes in symmetry (see tables 1 and 3). The same space groups appear due to Ψ_z tilts in structures with $l = 2n + 1$ and $l = 2n$ layers in perovskite-like slabs.

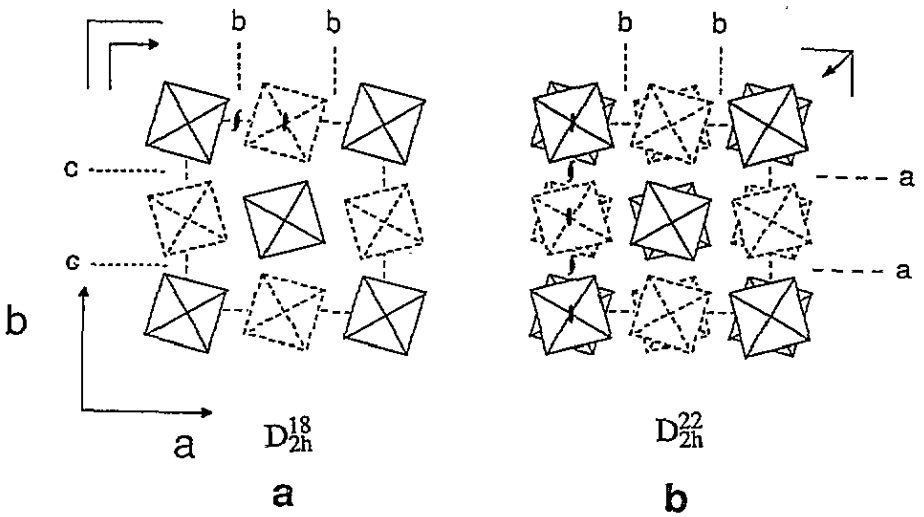

Figure 4. The structural distortions due to Φ_z and Ψ_z tilts: (a) the $(00\Psi_z)(00\Psi_z)$ tilt system, equal tilts around the c_0 axis in both slabs; (b) the $(00\Phi_z)(00\Phi_z)$ system. Some symmetry elements of space groups are shown.

3.2. Tilts of the $(00\Phi_z)$ kind

These lead to three different distortions of G_0. One of them, $(00\Phi_z)(00\Phi_z)$, is shown in figure 4(b). It corresponds to $G_1 = D_{2h}^{22} = Abaa$, $Z = 4$, $a = \sqrt{2}a_0$, $b = \sqrt{2}b_0$, $c = c_0$ (the standard symbol *Ccca* is used in table 1). The symmetry of the other two phases with $(002\Phi_z)(000)$ and $(00\Phi_{1z})(00\Phi_{2z})$ systems of tilts is listed in table 1. Φ_z tilts are induced by a τ_2 irrep of G_0 (see table 3).

3.3. Tilts of the Ψ and Φ kind

The situations with the rotation axes of the octahedra in the slab plane lead to more numerous tilt systems, which will be considered below for the case of Φ tilts. When a one-component Φ tilt takes place in both slabs the symmetry of the resultant space group G_i depends both on the phases of the tilts of the adjacent slabs, and on the axes of the tilts in the

Table 1. The symmetry of distorted phases arising due to octahedral tilts in crystals with an even number of layers in the perovskite-like slabs ($l = 2n$).

No	Symbols of tilts: 1st slab	2nd slab	Space group	Unit cell parameters: a	b	c	Z	Irrep of G_0	Remarks
1	000	000	D_{4h}^{17}—$I4/mmm$	a_0	a_0	c_0	2		
2	$00\Psi_z$ $00\Psi_z$	$00\Psi_z$ $00\bar{\Psi}_z$	D_{2h}^{18}—$Cmca$	c_0	$\sqrt{2}a_0$	$\sqrt{2}a_0$	4	τ_7	Figure 4(a)
3	$00\Psi_z$	000	D_{4h}^{5}—$P4/mbm$	$\sqrt{2}a_0$	$\sqrt{2}a_0$	c_0	4	τ_7	
4	$00\Psi_{z1}$	$00\Psi_{z2}$	D_{2h}^{9}—$Pbam$	"	"	"	4	τ_7	
5	$00\Phi_z$	$00\Phi_z$	D_{2h}^{22}—$Ccca$	$\sqrt{2}a_0$	c_0	$\sqrt{2}a_0$	4	τ_2	Figure 4(b)
6	$00\Phi_z$	000	D_{4h}^{3}—$P4/nbm$	$\sqrt{2}a_0$	$\sqrt{2}a_0$	c_0	4	τ_2	
7	$00\Phi_{z1}$	$00\Phi_{z2}$	D_{2h}^{4}—$Pban$	"	"	"	4	τ_2	
8	$\Phi 00$ $\Phi_1\Phi_2 0$	$\Phi 00$ $\Phi_1\Phi_2 0$	C_{2h}^{3}—$A112/m$	"	"	"	4	—	Figure 5(a)
9	$\Phi 00$	$0\bar{\Phi}0$	D_{4h}^{10}—$P4_2/mcm$	"	"	"	4	τ_6	Figure 5(b)
10	$\Phi\Phi 0$	$\bar{\Phi}\bar{\Phi}0$	D_{2h}^{21}—$Cmma$	$\sqrt{2}a_0$	c_0	$\sqrt{2}a_0$	4	τ_6	Figure 6(c)
11	$\Phi_1\Phi_2 0$	$\bar{\Phi}_2\bar{\Phi}_1 0$	D_{2h}^{3}—$Pccm$	$\sqrt{2}a_0$	$\sqrt{2}a_0$	c_0	4	τ_6	
12	$\Phi 00$	$0\Phi 0$	D_{4h}^{14}—$P4_2/mnm$	"	"	"	4	τ_4	Figure 5(c)
13	$\Phi\Phi 0$	$\Phi\Phi 0$	D_{2h}^{17}—$Cmcm$	c_0	$\sqrt{2}a_0$	$\sqrt{2}a_0$	4	τ_4	Figure 6(b)
14	$\Phi_1\Phi_2 0$	$\Phi_2\Phi_1 0$	D_{2h}^{12}—$Pnnm$	$\sqrt{2}a_0$	$\sqrt{2}a_0$	c_0	4	τ_4	
15	$\Phi\Phi 0$	$\Phi\bar{\Phi}0$	D_{4h}^{4}—$P4/nnc$	"	"	"	4	—	Figure 6(a)
16	$\Phi_1\Phi_2 0$	$\Phi_1\bar{\Phi}_2 0$	C_{2h}^{1}—$P112/m$	"	"	"	4	—	
17	$\Psi 00$	$\Psi 00$	D_{2h}^{13}—$Pmmn$	$2a_0$	a_0	c_0	4	—	
18	$\Psi 00$	$0\Psi 0$	D_{4h}^{9}—$P4_2/mmc$	$2a_0$	$2a_0$	c_0	8	—	
19	$\Psi\Psi 0$ $\Psi\Psi 0$	$\Psi\bar{\Psi}0$ $\Psi\Psi 0$	D_{2h}^{17}—$Cmcm$	$2\sqrt{2}a_0$	$2\sqrt{2}a_0$	c_0	16	—	
20	$\Psi_1\Psi_2 0$	$\Psi_1\Psi_2 0$	C_{2h}^{2}—$P112_1/m$	$2a_0$	$2a_0$	c_0	8	—	

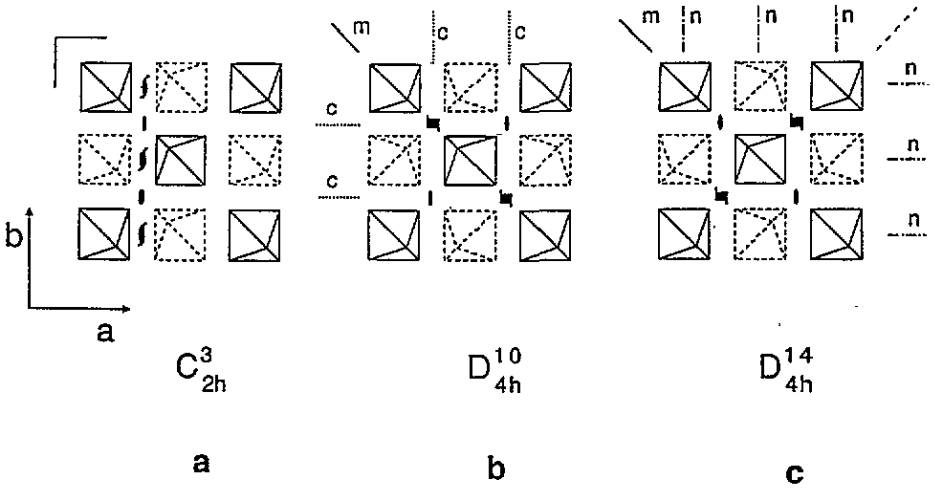

Figure 5. Three different tilt systems due to ($\Phi 00$) tilts in a slab: (a) the ($\Phi 00$)($\Phi 00$) system; (b) the ($\Phi 00$)($0\bar{\Phi}0$) system; (c) the ($\Phi 00$)($0\Phi 0$) system.

$[001]_0$ planes. Three possible cases that differ in symmetry are shown in figure 5. Some

symmetry elements of the space groups are included in figures 5 and 6 to aid the reader to distinguish the cases with different tilt axes and phases. In the first case, figure 5(a), the rotation axes of the Φ tilts are parallel in adjacent slabs and, irrespective of their phases, the tilt system $(\Phi 00)(\Phi 00)$ leads to the A-centred monoclinic group C_{2h}^3 (see table 1). The same group is produced for $(\Phi_1\Phi_2 0)(\Phi_1\Phi_2 0)$ distortion when Φ tilts around a_0 and b_0 are non-equal and are parallel in both slabs. When Φ tilts occur around a_0 in the first slab and b_0 in the adjacent one, the symmetry of the distorted structure depends on the tilt phases, as is clearly seen in figure 5(b, c). Figure 5(b) corresponds to the $(0\Phi 0)(0\bar{\Phi}0)$ tilt system and to $G_1 = D_{4h}^{10}$—$P4_2/mcm$, $Z = 4$. The tilts of $(\Phi 00)(0\Phi 0)$ type in figure 5(c) leads to another tetragonal group $G_1 = D_{4h}^{14}$—$P4_2/mnm$, $Z = 4$. The symmetry change $D_{4h}^{17}(Z = 2) \rightarrow D_{4h}^{14}$ $(Z = 4)$ corresponds to the appearance of two equal components (η, η) of the order parameter, which transforms in accordance with the $\tau_4(X_3^-)$ irrep of the K_{13} star [21]. The tilt systems $(\Phi 00)(0\bar{\Phi}0)$, $(\Phi\Phi 0)(\bar{\Phi}\bar{\Phi}0)$ and $(\Phi_1\Phi_2 0)(\Phi_2\Phi_1 0)$ are induced by τ_6 of G_0 (see table 3).

The distortion $(\Phi\Phi 0)(\Phi\bar{\Phi}0)$, with orthogonal $[110]_0$ axes of the Φ tilts in the slabs, also leads to a tetragonal structure D_{4h}^4 and the symmetry does not depend on the tilt phases: $(\Phi\Phi 0)(\bar{\Phi}\Phi 0)$ is also tetragonal. In contrast $(\Phi\Phi 0)(\Phi\Phi 0)$, figure 6(b), and $(\Phi\Phi 0)(\bar{\Phi}\bar{\Phi}0)$, figure 6(c), tilt systems with parallel axes lead to the different space groups D_{2h}^{17}—$Cmcm$, $Z = 4$, and D_{2h}^{21}—$Cmma$, $Z = 4$, correspondingly. These groups are B and A centred as is seen from figure 6(b, c). This means that the centring of the unit cell depends on the phases of the Φ tilts in adjacent slabs, but not on the odd or even number of octahedral layers in the slabs as stated repeatedly by Australian authors [22–25]. The tilt system $(\Phi\Phi 0)(\Phi\Phi 0)$ corresponds to the appearance of a single component $(\eta, 0)$ or $(0, \eta)$ of the same order parameter due to the $\tau_4(X_3^-)$ irrep [21]. With non-equal components of Φ tilts in a slab $(\eta_1 \neq \eta_2 \neq 0)$ the orthorhombic group becomes D_{2h}^{12}—$Pnnm$ with $Z = 4$. The other combinations of tilts and tilt systems due to Ψ tilts are presented in table 1.

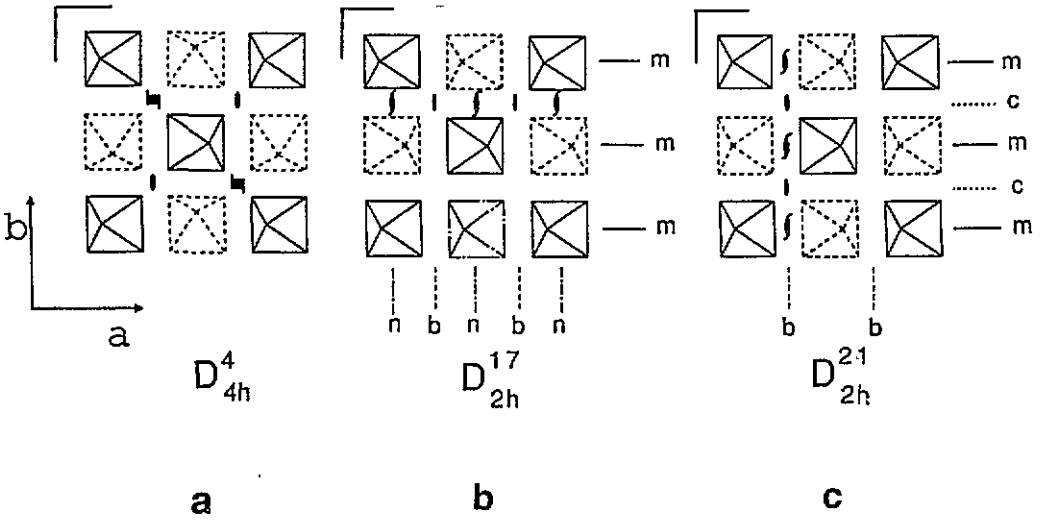

Figure 6. Three different tilt systems due to $(\Phi\Phi 0)$ tilts in a slab: (a) the $(\Phi\Phi 0)(\Phi\bar{\Phi}0)$ system; (b) the $(\Phi\Phi 0)(\Phi\Phi 0)$ system; (c) the $(\Phi\Phi 0)(\bar{\Phi}\bar{\Phi}0)$ system.

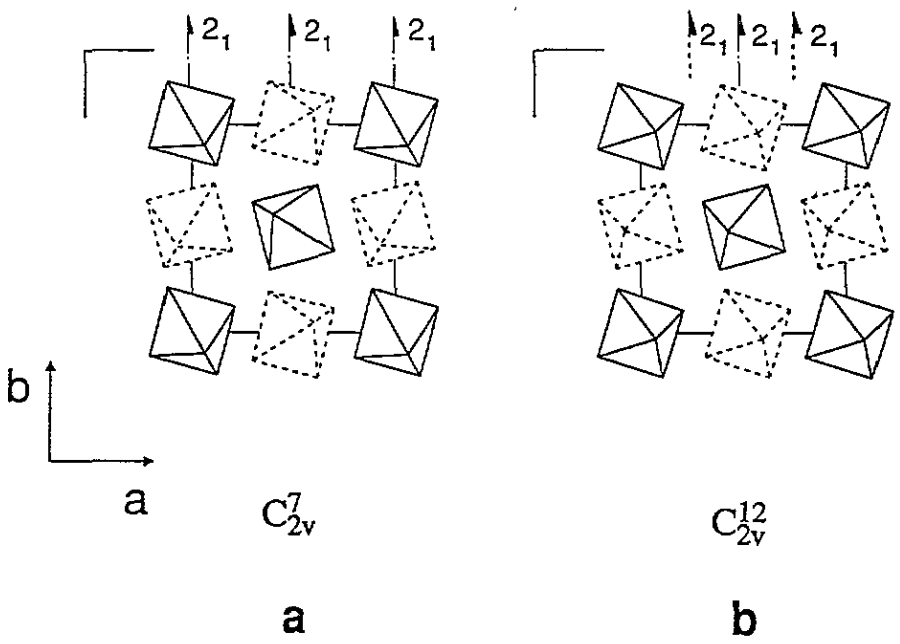

Figure 7. Two polar structures due to superpositons of (a) $(\Phi 00)(0\Phi 0)$ and (b) $(\Phi\Phi 0)(\Phi\Phi 0)$ with the $(00\Psi_z)(00\Psi_z)$ system of tilts (see the text).

3.4. Superposition of different kinds of tilt (Ψ_z, Ψ, Φ_z, Φ)

This leads to many complicated distortions of G_o. In contrast to crystals with odd-number perovskite-like slabs [9, 10], distortions in crystals with $l = 2n$ often lead to the loss of a symmetry centre. Two examples are shown in figure 7(a,b) for $(\Phi 0\Psi_z)(0\Phi\Psi_z)$ and $(\Phi\Phi\Psi_z)(\Phi\Phi\Psi_z)$ tilt systems, respectively. The structures in figure 7 are the results of superpositions of distortions presented in figure 5(c) and 6(b) with the $(00\Psi_z)(00\Psi_z)$ tilt system similar to figure 4(a). Both structures are polar, with the main axis along b in figure 7 (see table 2). They may appear in the course of successive (or triggered) PTs where two different order parameters participate. As was mentioned above, the parameters can be considered as tilts due to the condensation of the soft librational lattice modes τ_4 and τ_7 [10–12, 21].

It is worthwhile to mention that other polar phases can appear when the same Φ-tilt systems are superimposed with $(00\Psi_z)(000)$ or $(00\Psi_{1z})(00\Psi_{2z})$ systems. In the case of $(\Phi 0\Psi_z)(0\Phi 0)$ we obtain the C-centred orthorhombic space group C_{2v}^{14}—$Cmm2$, $Z = 8$ with the polar axis along one of the $[110]_0$ directions of G_o. When $\Psi_z \to 0$ we obtain the transformation from C_{2v}^{14} to D_{4h}^{14} (figure 5(c)). Another case $(\Phi\Phi\Psi_z)(\Phi\Phi 0)$ leads to the primitive group C_{2v}^{2}—$Pmc2_1$, $Z = 4$, and the polar axis is now parallel to $[110]_0$ (see table 2). This distortion can also appear in some sequences of structural PTs.

It is interesting to mention also that the structure in figure 7(b) becomes non-polar when the sign of the Ψ tilt is changed in one of the slabs (see table 2). Similar polar–non-polar transformation takes place with the $(\Phi\Phi\Psi_z)(\bar{\Phi}\bar{\Phi}\Psi_z)$ system, but does not exist with $(\Phi 0\Psi_z)(0\Phi\Psi_z)$ and $(\Phi 0\Psi_z)(0\Phi\bar{\Psi}_z)$ tilts. Both these latter structures are polar (see figure 7(a) and table 2). The structure in figure 7(b) will be discussed below in more detail. We did not consider many other examples of superpositions: $(00\Psi_z)(000)$; $(00\Psi_{1z})(0\Phi\Psi_{2z})$;

Table 2. Structure distortions of G_0 due to superposition of different kinds of tilt (structures with even layers in slabs, $l = 2n$).

No	Symbols of tilts		Space group	Unit cell parameters			Z	Irrep of G_0	Remarks
	1st slab	2nd slab		a	b	c			
1	$\Psi\Phi 0$ $\Psi 0\Psi_z$ $\Psi\Psi\Psi_z$	$\Psi\Phi 0$ $\Psi 0\Psi_z$ $\Psi\Psi\Psi_z$	C_{2h}^2—$P112_1/m$	$2a_0$	$2a_0$	c_0	8		
2	$\Psi\Phi 0$	$\Phi\Psi 0$	D_{2h}^{20}—$Cccm$	$2\sqrt{2}a_0$	$2\sqrt{2}a_0$	c_0	16		
			C_{2h}^1—$P112/m$	$2a_0$	$2a_0$	c_0	8		
3	$\Phi 0\Psi_z$ $\Phi_1\Phi_2\Psi_z$	$\Phi 0\Psi_z$ $\Phi_1\Phi_2\Psi_z$	C_{2h}^2—$P112_1/m$	$\sqrt{2}a_0$	$\sqrt{2}a_0$	c_0	4		
4	$\Phi 0\Psi_z$ $\Phi 0\Psi_z$	$0\Phi\Psi_z$ $0\Phi\bar{\Psi}_z$	C_{2v}^7—$Pmn2_1$	c_0	$\sqrt{2}a_0$	$\sqrt{2}a_0$	4	$\tau_4 \otimes \tau_7$	Figure 7(a)
5	$\Phi\Phi\Psi_z$	$\Phi\Phi\bar{\Psi}_z$	D_{2h}^{16}—$Pnma$	$\sqrt{2}a_0$	$\sqrt{2}a_0$	c_0	4	$\tau_4 \otimes \tau_7$	
6	$\Phi\Phi\Psi_z$	$\Phi\Phi\Psi_z$	C_{2v}^{12}—$Cmc2_1$	$\sqrt{2}a_0$	c_0	$\sqrt{2}a_0$	4	$\tau_4 \otimes \tau_7$	Figure 7(b)
7	$\Phi_1\Phi_2\Psi_z$	$\Phi_2\Phi_1\Psi_z$	C_{2v}^7—$Pmn2_1$	c_0	$\sqrt{2}a_0$	$\sqrt{2}a_0$		$\tau_4 \otimes \tau_7$	
8	$\Phi 0\Psi_z$	$0\Phi 0$	C_{2v}^{14}—$Amm2$	c_0	$2a_0$	$2a_0$	8	$\tau_4 \otimes \tau_7$	
9	$\Phi\Phi\Psi_z$	$\Phi\Phi 0$	C_{2v}^2—$Pmc2_1$	c_0	$\sqrt{2}a_0$	$\sqrt{2}a_0$	4	$\tau_4 \otimes \tau_7$	
10	$\Phi 0\Psi_z$	$0\bar{\Phi}\Psi_z$	C_{2v}^4—$Pma2$	"	"	"	4	$\tau_6 \otimes \tau_7$	
11	$\Phi\Phi\Psi_z$	$\bar{\Phi}\bar{\Phi}\Psi_z$	D_{2h}^{11}—$Pbcm$	"	"	"	4	$\tau_6 \otimes \tau_7$	
12	$\Phi\Phi\Psi_z$	$\bar{\Phi}\bar{\Phi}\bar{\Psi}_z$	C_{2v}^{15}—$Abm2$	"	"	"	4	$\tau_6 \otimes \tau_7$	
13	$\Phi_1\Phi_2\Psi_z$	$\bar{\Phi}_1\bar{\Phi}_2\Psi_z$	C_{2v}^4—$Pma2$	"	"	"	4	$\tau_6 \otimes \tau_7$	
14	$\Psi 0\Psi_z$ $\Psi\Psi\Psi_z$	$0\Psi\Psi_z$ $\bar{\Psi}\bar{\Psi}\Psi_z$	C_{2v}^{16}—$Ama2$	$2\sqrt{2}a_0$	$2\sqrt{2}a_0$	c_0	16		
15	$\Phi 0\Phi_z$ $\Phi_1\Phi_2\Phi_z$	$0\Phi\Phi_z$ $\Phi_2\Phi_1\Phi_z$	C_{2h}^5—$P2_1/n11$	$\sqrt{2}a_0$	$\sqrt{2}a_0$	c_0	4	$\tau_4 \otimes \tau_2$	
16	$\Phi\Phi\Phi_z$	$\Phi\Phi\Phi_z$	C_{2h}^6—$B2/b11$	"	"	"	4	$\tau_4 \otimes \tau_2$	
17	$\Phi 0\Phi_z$ $\Phi_1\Phi_2\Phi_z$	$0\bar{\Phi}\Phi_z$ $\bar{\Phi}_2\bar{\Phi}_1\Phi_z$	C_{2h}^4—$P12/c$	"	"	"	4	$\tau_6 \otimes \tau_2$	
18	$\Phi\Phi\Phi_z$	$\bar{\Phi}\bar{\Phi}\Phi_z$	D_{2h}^8—$Pcca$	"	"	"	4	$\tau_6 \otimes \tau_2$	
19	$\Phi\Phi\Phi_z$	$\Phi\Phi 0$	C_{2h}^4—$P2/c11$	c_0	$\sqrt{2}a_0$	$\sqrt{2}a_0$	4	$\tau_4 \otimes \tau_2$	
20	$\Phi 0\Phi_z$	$0\Phi 0$	C_{2h}^3—$C2/m11$	$2a_0$	$2a_0$	c_0	8	$\tau_4 \otimes \tau_2$	
21	$\Psi 0\Phi_z$ $\Psi\Phi\Phi_z$	$0\Psi\Phi_z$ $\Phi\Psi\Phi_z$	C_{2h}^6—$C12/c1$	$2\sqrt{2}a_0$	$2\sqrt{2}a_0$	c_0	16		
22	$\Psi 0\Phi_z$	$\Psi 0\Phi_z$	C_{2h}^5—$P112_1/a$	$2a_0$	$2a_0$	c_0	8		

$(00\Phi_z)(000)$ and $(00\Phi_{1z})(0\Phi\Phi_{2z})$ tilt systems with many other Φ and Ψ tilts along a_0 and b_0 axes. Most cases are not too complicated to develop, if needed.

At first glance it is surprising that polar phases appear due to superpositions of centrosymmetric primitive distortions, but this does not contradict the well known Curie principle. When two or more combinations of symmetry elements (two or more space groups, a space group and an external field, etc) are superimposed the combined system retains only the common symmetry elements located at the same lattice sites. Similar non-centrosymmetrical cases have been also met in the distorted perovskites and in A_2BX_4-type crystals [3, 10].

Many other cases of complex distortions have been considered. Some of them are listed in table 2. We restrict ourselves to the cases where either one or zero tilts of any kind may appear along a_0, b_0 and c_0 axes of G_0. Some of these cases such as $(\Psi_1\Psi_2\Psi_z)(\Psi_1\Psi_2\Psi_z)$ and $(\Psi\Phi\Psi_z)(\Psi\Phi\Psi_z)$ lead to $P\bar{1}$ or $P1$ groups and large unit cells. These cases are not presented in table 2. We did not consider either the superpositions of Φ and Ψ tilts along the same (a_0 or b_0) axes or tilt systems with different sets of tilts in adjacent slabs.

4. Discussion

As was mentioned in section 1, there exist two methods to perform the symmetry analysis of structure distortions in this type of crystal. The group-theoretical method gives all possible group–subgroup changes due to active irreps of G_0 [29], but the determination of atomic positions in the distorted structure G_i needs a more sophisticated study and is not usually performed. It has been done only in a restricted number of cases [26, 27], when the structure changes corresponding to $G_0 \rightarrow G_i$ are known from experiment or other sources.

On the other hand, the crystallographic method used in this paper enumerates all possible symmetry changes due to the restricted number of definite simple distortions: four kinds of tilt in our case. The results of the analysis have no direct relation to the group-theoretical ones and it is impossible to determine by which active representation of G_0 the tilt system is induced. However, both methods make tables of the possible symmetry changes of G_0 redundant. The comparison of these tables helps to find the active irreps that determine the structural changes due to the definite distortion in the crystal under consideration.

4.1. Sequences of PTs

Fortunately, the group-theoretical analysis of $G_0 = D_{4h}^{17}$—$I4/mmm$ has been performed many times [11, 12, 26, 27]. In most cases these papers have been devoted to the study of the structural phase transitions in the A_2BX_4 perovskite-like crystals. As far as we know, full tables of the G_0 subgroups have been enumerated only in sources to which it is difficult to have access [28, 41]. For our purpose, the symmetry changes induced by the irreps of the $K_{13}(X)$ star of G_0 are needed. These data, first published in [28] and partially reproduced in [30], are shown in table 3.

In order to summarize the resulting phases due to tilts in perovskite-like crystals with odd ($l = 2n + 1$) and even ($l = 2n$) layers in slabs of octahedra, the last column in table 3 was added. It is shown there, for crystals with $l = 2n + 1$ and $l = 2n$, which kind of tilt induces the symmetry changes equivalent to those corresponding to definite $\tau_i(K_{13})$, in Kovalev's notation [19]. From inspection of the table one easily verifies that the tilt systems due to Φ and Ψ_z tilts in crystals with $l = 2n + 1$ give the same symmetry changes as τ_3, τ_5 and τ_7. The Φ_z tilts in crystals with $l = 2n$ belong to τ_2 but in the cases of odd layers in slabs Φ_z tilts belong to the same irrep as Ψ_z ones and lead to the same symmetry changes. Irrep τ_7 is met three times at the X point of the Brillouin zone of A_2BX_4 crystals [26] and probably Φ_z and Ψ_z tilts in multilayered crystals with $l = 2n + 1$ are determined by different modes of the same symmetry.

As for the crystals with an even number of octahedral layers in the slabs, the tilt systems due to Ψ_z, Φ_z and Φ kinds lead to the same symmetry changes as τ_7, τ_2 and τ_4, τ_6, respectively. As was seen in table 1 and figures 5 and 6, Φ tilts due to changes of the tilt phases in the neighbouring slabs can lead to two different sequences of PTs. These are new cases of the distortional polytypism considered earlier [8, 10]. The PT sequences that can be induced by τ_4 and τ_5 are

$$D_{4h}^{17} \xrightarrow{\tau_4(0,\eta)} D_{2h}^{17} \xrightarrow{\tau_4(\eta,\eta)} D_{4h}^{14} \xrightarrow{\tau_4(\eta_1,\eta_2)} D_{2h}^{12} \tag{1}$$

$$D_{4h}^{17} \xrightarrow{\tau_6(0,\eta)} D_{2h}^{21} \xrightarrow{\tau_6(\eta,\eta)} D_{4h}^{10} \xrightarrow{\tau_6(\eta_1,\eta_1)} D_{2h}^{3}. \tag{2}$$

Both (1) and (2) correspond to transformations between tetragonal–orthorhombic–tetragonal–orthorhombic phases. They lead to the same unit-cell multiplication and

Table 3. The symmetry of distorted phases induced by irreducible representations of the $K_{13}(X)$ star in crystals belonging to $G_o = I4/mmm$ for $l = 2n$ and $l = 2n + 1$.

	$\tilde{\eta} = (0, \eta)$		$\bar{\eta} = (\eta, \eta)$		$\tilde{\eta} = (\eta_1, \eta_2)$		Kinds of tilt in crystals with l octahedral layers in slabs
τ_i	G_i	Orientations of planes in G_o	G_i	Orientations of planes in G_o	G_i	Orientations of planes in G_o	
τ_1	D_{2h}^{19}—*Cmmm*	m_1–(001); m_2–(110)	D_{4h}^{1}—*P4/mmm*	m_1–(001); m_2–(100)	D_{2h}^{1}—*Pmmm*	m_1–(110); m_2–(1$\bar{1}$0)	—
τ_2	D_{2h}^{22}—*Ccca*	c_1–(001); c_2–(110)	D_{4h}^{3}—*P4/nbm*	*b*–(110); *m*–(100)	D_{2h}^{4}—*Pban*	*b*–(110); *a*–($\bar{1}$10)	Φ_z for $l = 2n$
τ_3	D_{2h}^{18}—*Ccma*	*c*–(001); *m*–(110)	D_{4h}^{16}—*P4$_2$/ncm*	*c*–(110); *m*–(100)	D_{2h}^{10}—*Pccn*	c_1–(110); c_2–($\bar{1}$10)	Φ, Φ for $l = 2n + 1$
τ_4	D_{2h}^{17}—*Cmcm*	m_1–(001), ($\bar{1}$00); c_2–(110)	D_{4h}^{14}—*P4$_2$/mnm*	*n*–(110); *m*–(100), (001)	D_{2h}^{12}—*Pnnm*	*n*–(110), ($\bar{1}$10); *m*–(001)	Φ, Φ for $l = 2n$
τ_5	D_{2h}^{20}—*Ccem*	*c*–(001), (110); *m*–($\bar{1}$10)	D_{4h}^{12}—*P4$_2$/nnm*	*n*–(110), (001); *m*–(100)	D_{2h}^{2}—*Pnnn*	*n*–(110), ($\bar{1}$10), (001)	Φ, $\bar{\Phi}$ for $l = 2n + 1$
τ_6	D_{2h}^{21}—*Cmma*	*m*–(001), (110); *a*–($\bar{1}$10)	D_{4h}^{10}—*P4$_2$/mcm*	*m*–(100), (001); *n*–(110)	D_{2h}^{3}—*Pccm*	*c*–(110), (1$\bar{1}$0); *m*‖ (001)	Φ, $\bar{\Phi}$ for $l = 2n$
τ_7	D_{2h}^{18}—*Ccma*	m_1–(001); *c*–(110)	D_{4h}^{5}—*P4/mbm*	*m*–(100), (001); *b*–(110)	D_{2h}^{9}—*Pbam*	*m*–(001); *b*–(110)	Ψ_z, Φ_z for $l = 2n + 1$ Ψ_z for $l = 2n$
τ_8	D_{2h}^{17}—*Ccmm*	*m*–(110), (001); *c*–($\bar{1}$10)	D_{4h}^{7}—*P4/nmm*	*m*–(110), (100); *n*–(001)	D_{2h}^{13}—*Pmmn*	*m*–(110), (1$\bar{1}$0); *n*–(001)	—

orientation of the axis. Many examples of more complex sequences can be considered using the results of table 2. Some cases of superposition of different tilt systems are listed there. The symmetry changes in these cases can be found taking the direct product of two irreps, $\tau_4 \otimes \tau_7$, for example. A similar analysis for A_2BX_4 ($l = 1$) crystals was done earlier [11, 12]. The direct products of irreps in table 2 are the results of our symmetry analysis due to the superpositions of different tilt systems, and should be checked by the group-theoretical method.

An additional question consists in performing the analysis of the lattice vibrations for crystals with a defiite prototype structure G_0. The aim of the analysis is the determination of the normal vibrations, which have equivalent symmetry properties to the G_0 irreps involved, since they can be the condensing soft modes at the PT. For A_2BX_4 crystals the problem has been solved earlier [26, 27]. It was shown that there exist librational modes at the X point of the zone that have the same symmetry as the τ_3, τ_5 and τ_7 irreps. On the other hand, the problem has not been solved for more complex crystals with $l > 1$. However, it can be proposed that the irreps listed in table 3 (except for τ_1 and τ_8) may induce in the layered crystals PTs of displacive type and, correspondingly, the soft modes may be found.

4.2. Comparison to experiments

Examples of well studied PTs in perovskite-like crystals with an even number of octahedral layers in the slabs are very limited, in spite of the large number of crystals belonging to the considered series, and specially to the anion-deficient related crystals. It was found that many representatives of the Aurivillius-type crystals are ferroelectrics and some of them present also PTs of unknown nature below the Curie temperature [31–33]. These PTs have not been investigated in detail. Their nature can be very different: positional order–disorder processes, ionic conductivity, non-stoichiometry, etc, but the mechanism of tilting cannot be excluded and it seems to be one of the most probable.

It was also found that many crystals of both the Aurivillius and Ruddlesden–Popper series have the unit-cell parameters a and b nearly equal to $\sqrt{2}a_0$ of G_0 and $Z = 4$, but x-ray powder data did not allow us to distinguish the type of distortion [31–33]. In these cases the distorted structures have been often considered as having an F-centred unit cell with $a \simeq b \simeq \sqrt{2}a_0$ and $c \simeq c_0$, which sometimes had additional polar distortions.

The structures of a few substances have been solved for single crystals. Three known examples, $Ca_3Ti_2O_7$ [38], Bi_3TiNbO_9 [25] and $Bi_2SrTa_2O_9$ [24] (table 4), have the same space group, C_{2v}^{12}—$Cmn2_1$, or $A2_1am$ in the notations of [24] and [25]. This is the same polar group as was determined above (see section 3.4 and figure 7(b)) as the result of superposition of the $(\Phi\Phi 0)(\Phi\Phi 0)$ and $(00\Psi_z)(00\Psi_z)$ systems of tilts (table 2, No 6). The structures of the crystals mentioned above really contain the anion displacements corresponding to the mentioned system of tilts. Polar distortions due both to polar shifts of central atoms inside the octahedra and the displacements of A atoms in the perovskite-like slabs along the polar $[110]_0$ direction are superimposed on the system of tilts. The values of Φ and Ψ_z angles are different because of the different irreps involved (see table 3). Their values are usually less than 10° [24, 25, 38].

The crystal $Rb_3Cd_2Cl_7$ has been studied with different experimental techniques such as heat capacity, birefringence and x-ray powder analysis [21]. Two phase transitions have been found from tetragonal (G_0) to orthorhombic and from orthorhombic to tetragonal phases upon lowering of temperature (see table 4). A partial crystallographic analysis, similar to the one performed in this work, has been done [21]. It was assumed that the sequence of PTs in the crystal corresponds to expression (1), i.e. it is induced by the τ_4 irrep. The expression (2), as mentioned above (see tables 1 and 3), leads to the same point-symmetry changes

Table 4. Experimental data and proposed tilt systems in the structures of the studied perovskite-like crystals.

Substance	Space group	Lattice constants, *A*			*Z*	Proposed tilt systems	
		a	*b*	*c*			
$Bi_2SrTa_2O_9$	$A2_1am$	5.5306	5.5344	24.984	4	$(\Phi\Phi\Psi_z)(\Phi\Phi\Psi_z)$	[24]
Bi_3TiNbO_9	$A2_1am$	5.4398	5.3941	25.099	4	$(\Phi\Phi\Psi_z)(\Phi\Phi\Psi_z)$	[23, 25]
$Bi_2SrNb_2O_9$	$A2_1am$	5.5094	5.5094	25.098	4	$(\Phi\Phi\Psi_z)(\Phi\Phi\Psi_z)$	[24]
$Rb_3Cd_2Cl_7$	$I4/mmm$	5.197	—	26.366	4	—	[21], $T > 214$ K
	$Bbmm$	7.341	7.341	26.235	4	$(\Phi\Phi0)(\Phi\Phi0)$	[21], $213.6 > T > 172$ K
	$P4_2/mnm$	7.339	—	26.157	4	$(\Phi00)(0\Phi0)$	[21], $T < 172$ K
$Ca_3Ti_2O_7$	$Ccm2_1$	5.4172	19.5169	5.4234	4	$(\Phi\Phi\Psi_z)(\Phi\Phi\Psi_z)$	[38]
$SrTb_2Fe_2O_7$	$P4_2/mnm$	5.506	—	19.659	4	$(\Phi00)(0\Phi0)$	[34]
$SrLa_2Sc_2O_7$	$Fmmm$	5.7818	5.7367	20.534	4	—	[37]

and to the same macroscopic characteristics of the PTs. Single-crystal x-ray analysis may distinguish between these two versions, deserving new experiments.

The data of Samaras *et al* [34] on some complex ferrites with the perovskite-like double-layered structure (see figure 1(b)) may be in agreement with the PT sequence proposed in [21]. In one of the substances, $SrTb_2Fe_2O_7$, the structure was slightly distorted and the Rietveld analysis of the data gave the best results for the D_{4h}^{14}—$P4_2/mnm$ space group, which is the G_2 phase in expression (1). The atomic coordinates published in [34] show that the main distortions are the octahedral tilts of the proper system. According to the 'model structure' shown in figure 5(c) the oxygen atoms O(1) linking the octahedra between $(001)_0$ layers in a slab and the O(2) ones on the external tops of the slabs have shifts along $[110]_0$ equal in value and opposite in sense. One half of the O atoms in the planes of the octahedral layers, (O(3) in G_0), are shifted along $\pm z_0$, the other half do not change their coordinates, in a first approximation. Just these displacements are the largest ones in the structure of $SrTb_2Fe_2O_7$ [34]. The displacements by $\pm\Delta z$ of Fe atoms from the octahedral centres provide evidence of the antiferroelectric nature of the crystal structure. It is worthwhile to mention also the possible structural PTs at high temperature present in this crystal, in accordance with the expected PT sequence (1).

The main positional changes of the anions forming the octahedra in layered perovskite-like crystals can be found in a similar way for any distorted phase listed in tables 1 and 2. In many cases the directions of the A-cation displacements can be found by taking account of the site symmetry and the form of the anion polyhedra around these ions in the distorted structure. We will consider as an example the first PT from (1): $D_{4h}^{17} \rightarrow D_{2h}^{17}$ (see table 1, line 13 and figure 6(b)). This corresponds to two Φ-tilt components in the plane of the two layered octahedral slabs for an $A_3B_2X_7$ crystal. There exist two types of A atom in the initial phase G_0. Atoms A_1 are located inside the slabs in positions with $Z = 12$ having the site symmetry (a) $4/mmm$. According to international tables for x-ray crystallography it is convenient to accept this point as the origin of the coordinate system: (000). A_2 atoms are located between slabs in positions (e) $4mm$ with $Z = 9$ and have the coordinates $(00z_0)$. After the PT to $G_1 = Cmcm$ a new coordinate system appears, $z_0 \rightarrow x_1$, $[110]_0 \rightarrow y_1$, $[1\bar{1}0]_0 \rightarrow z_1$, and the position of the origin also changes. Atoms A_1 and A_2 are located now in positions with site symmetry mm and m correspondingly. This conclusion can be easily made from the analysis of displacements for X atoms in their surroundings (see figure 6(b)). A_1 atoms are located now on the intersection of the two m planes and may change their coordinate $\pm\Delta y_1$ along this line; A_2 atoms are located on an m plane orthogonal to x_1 and may have displacements $\pm\Delta y_1$ and $\pm\Delta z_1$ in the plane. These displacements of A atoms plus those for two types of X atom can be used in the process

of structural analysis as free parameters of the trial model. X-ray- or neutron-diffraction experiments on powder samples are frequently performed now in the course of the search for new representatives of layered crystals, specially as HTSCs and related materials [39–41]. It is well known that some series of HTSCs belong to anion-deficient versions of the Aurivillius and Ruddlesden–Popper ones [35, 39]. In the course of structural research many examples have been found where the atomic positions have shifted to the partially occupied ones and have led to substantial lowering of the reliability (R) factors (see, for example, [36]).

At least in some cases the trial models could help to confirm or exclude one of the possible reasons for this peculiarity. Also, one may suspect that some other representatives of layered crystals with tolerance factors beyond the stability range of G_o (see [42]) will have distorted structures in some temperature region.

5. Summary

The crystallographic analysis of structural distortions caused by octahedral tilts in multilayered perovskite-like crystals with even octahedral layers in slabs has been performed. Two series of these crystals were considered: Aurivillius and Ruddlesden–Popper ones [17, 18] (figure 1). Four kinds of octahedral tilt are possible in the multilayered perovskite-like slabs: Ψ, Φ, Ψ_z, and Φ_z (figure 2).

An artificial method to simplify the symmetry analysis has been used. This allowed us to determine the symmetry of the distorted phases due to both a single kind of tilt (table 1) and to superpositions of different tilts along the unit-cell axis of the prototype structure $G_o = D_{4h}^{17} = I4/mmm$ (table 2). It was shown that many polar distortions appear when Φ and Ψ tilts are superimposed. In particular, for the $(\Phi\Phi\Psi_z)(\Phi\Phi\Psi_z)$ system of tilts (see No 6 in table 2), the group obtained was $Cmc2_1$ ($Z = 4$). The same group has been found in some crystals with $l = 2$ (table 4). These crystals are pyroelectrics and some additional polar distortions are superimposed on the mentioned system of tilts. These polar distortions alone can never lead to the complex tilt system: superpositions of the G_o group and one of the polar vectors directed along $[110]_0$ can never lead to the multiplication of the unit cell. However, a combination of the polar mode and one of the octahedral rotational modes can induce another octahedral rotational mode. Which one is the softest mode cannot be determined from group theory. Nobody knows at present whether these three modes are condensed at the same temperature.

The data published earlier [9–12] for the structural distortions due to tilts in A_2BX_4 crystals with K_2MgF_4-type structure ($l = 1$) have been reproduced also for crystals with $(2n + 1)$-layered octahedral slabs. It is easy to show that the symmetry of G_i due to Ψ, Φ and $\Psi_z \equiv \theta$ tilts and their superpositions does not change in the structures with $2n + 1$ layered slabs. Moreover, Φ_z tilts can appear in these crystals and lead to the same symmetry changes as the Ψ_z tilts. This means that both tilt systems belong to the same irrep τ_7 of G_o (see table 3). In A_2BX_4 crystals the irrep τ_7 is met three times at the X point of the Brillouin zone [26, 27]. Therefore one may expect that in crystals with multilayered slabs few librational modes will have the same symmetry τ_7. In this case these modes should interact and appear together in crystals with $l = 2n + 1$. In crystals with $l = 2n$ these tilts (Ψ_z and Φ_z) belong to different irreps (table 3). According to the published structural data, the superposition of the Ψ_z and Φ_z tilts takes place in the $Bi_4Ti_3O_{12}$ crystal belonging to Aurivillius phases with $l = 3$ [22, 24]. It could be mentioned here that it will be necessary to consider and determine the symmetry vectors for lattice modes in the future.

On the base of the system of tilts presented in tables 1 and 2, the directions and signs of atomic displacements can be found for all anions with respect to their sites in G_0. In many cases the displacements of A cations can also be estimated qualitatively. These displacements, combined with the unit-cell parameters and localizations of the symmetry elements in the G_i space group, form the set of data that was called above the 'trial model' for the structural analysis of the layered perovskite-like crystals. Some series of HTSCs (Tl_2 and Bi_2 series, for example) are the anion-deficient versions of the considered crystals with $l = 2n$, $l = 2n + 1$ and $G_0 = I4/mmm$. We hope that the results of this paper will be useful for the structural analysis of new layered crystals.

Acknowledgments

One of the authors (KA) acknowledges the Caja de Ahorros de la Inmaculada and CSIC for the financial support of his stay at ICMA in Zaragoza. This work was also supported partially by the Russian Foundation for Fundamental Research (project N93-2-2425) and by the Spanish CICYT (project PB 92-1077 and project MAT 93-0240-C04-04).

References

[1] Glazer A M 1972 *Acta Crystallogr.* B **28** 3384; 1975 *Acta Crystallogr.* A **31** 256
[2] Aleksandrov K S 1976 *Ferroelectrics* **14** 801; 1978 *Ferroelectrics* **20** 61; 1976 *Kristallographia* **21** 249
[3] Aleksandrov K S, Anistratov A T, Beznosikov B V and Fedoseeva N V 1981 *Phase Transitions in ABX_3 Crystals of Halide Compounds* (Novosibirsk: Nauka) (in Russian)
[4] Aleksandrov K S and Misjul'S V 1981 *Kristallographia* **26** 1074
[5] Armstrong R 1980 *Phys. Rep.* **57** 343
[6] Sutton M and Armstrong R 1983 *Phys. Rev.* B **27** 1937
[7] Deblieck R, Van Tandeloo G, Van Landuytz J and Amelinckx S 1985 *Acta Crystallogr.* B **41** 319
[8] Aleksandrov K S 1987 *Kristallographia* **32** 347
[9] Aleksandrov K S 1987 *Kristallographia* **32** 937
[10] Aleksandrov K S, Beznosikov B V and Misjul'S V 1987 *Phys. Status Solidi* a **104** 529
[11] Hatch D M and Stokes H T 1987 *Phys. Rev.* **35** 8509
[12] Hatch D M, Stokes H T, Aleksandrov K S and Misjul'S V 1989 *Phys. Rev.* B **39** 9282
[13] Bulou A and Nouet J 1982 *J. Phys. C: Solid State Phys.* **15** 183
[14] Aleksandrov K S, Emelyanova H S, Misjul'S V and Kokov J T 1985 *Solid State Commun.* **53** 835
[15] Schafer A D, Shabanov V F and Aleksandrov K S 1986 *JETP Lett.* **43** 491
[16] Axe J, Mouden A, Helmwein D, Cox D, Moharity K, Moodenbauch A and Xu X 1989 *Phys. Rev. Lett.* **62** 2751
[17] Ruddelsden S N and Popper P 1957 *Acta Crystallogr.* **10** 538; 1958 *Acta Crystallogr.* **11** 54
[18] Aurivillius B 1949 *Ark. Kemi* **1** 463, 499; 1950 *Ark. Kemi* **2** 519
[19] Kovalev O V 1986 *Irreducible and Induced Representations and Co-representations of Fedorov Groups* (Moscow: Nauka)
[20] Miller S C and Love W F 1967 *Tables of Irreducible Representations of Space Groups and Co-representations of Magnetic Space Groups* (Boulder, CO: Pruett)
[21] Aleksandrov K S, Kokov J T, Melnivova S V, Misjul' S V and Flerov J N 1988 *Fiz. Tverd. Tela* **30** 3652
[22] Withers R, Thompson J and Rae A 1991 *J. Solid State Chem.* **94** 404
[23] Thompson J, Rae A D, Withers R and Craig D 1991 *Acta Crystallogr.* B **47** 174
[24] Rae A D, Thompson J, Withers R and Willis A 1990 *Acta Crystallogr.* B **46** 474
[25] Rae D, Thompson J and Withers R 1992 *Acta Crystallogr.* B **48** 418
[26] Petzelt J 1975 *J. Phys. Chem. Solids* **36** 1005
[27] Geick R and Strobel K 1977 *J. Phys. C: Solid State Phys.* **10** 4221
[28] Naish V and Syromjatnikov B 1977 *Manuscript deposited with All-Union Inst. of Scientific Information* No 486
[29] Landau L D and Lifshitz E M 1980 *Statistical Physics* (New York: Pergamon) part 1

[30] Aleksandrov K, Beznosikov B and Misjuhl'S V 1986 *Institute of Physics, Siberian Department USSR Academy of Sciences Reprint* N381F
[31] Subbarao E 1973 *Ferroelectrics* 5 267
[32] Gungaly P and Rao C N R 1984 *J. Solid State Chem.* **53** 193
[33] Smolensky G, Bokov V, Isupov V, Krainik N and Sokolov A 1984 *Ferroelectrics and Related Materials* (New York: Gordon and Breach)
[34] Samaras D, Collomb A and Joubert J 1973 *J. Solid State Chem.* 7 337
[35] Raveau B, Mishel C and Hervieu B 1990 *Studies of High-temperature Superconductivity* vol 2, ed A Narlikar (New York: Nova) p 1
[36] Fu W and Helmholdt R 1992 *Mater. Res. Bull.* **27** 1371
[37] Kim J S, Kawaji H, Itoh M and Wakammta T 1992 *Mater. Res. Bull.* **27** 1193
[38] Elcombe M, Kisi E, Hawkins K, White T, Goodman P and Matheson S 1991 *Acta Crystallogr.* B 47 305
[39] Felner J, Hechel D, Yakoby E, Hilscher G, Holubar T and Schaudy G 1993 *Phys. Rev.* B **47** 12 190
[40] Frit B and Mercurio J 1992 *J. Alloys Compounds* **188** 27
[41] Stokes H T and Hatch D M 1988 *Isotropy Subgroups of the 230 Crystallographic Space Groups* (Singapore: World Scientific)
[42] Poix P 1980 *J. Solid State Chem.* **31** 95